文章编号: 1007 - 1482(2005)04 - 0199 - 06 ·特邀综述·

Twin characterisation using 2D and 3D EBSD

M. D. NAVE[1], J. J. L. MULDERS[2], A. GHOLINIA[3]

(1. Oxford Instruments, P. O. Box 9094, St Albans Park, Vic. 3219 Australia; 2. FEI Electron Optics, Building AAE, PO 60080, 5600 KA, Eindhoven, The Netherlands; 3. HKL Technology A/S, Majsmarken 1, Hobro, DK9500, Denmark)

Abstract: Electron backscatter diffraction (EBSD) is a superior technique for twin characterisation due to its ability to provide highly detailed classification (by generation, system and variant) of a significant number of twins in a relatively short time. 2D EBSD is now widely used for twin characterisation and provides quite good estimates of twin volume fractions under many conditions. Nevertheless, its accuracy is limited by assumptions that have to be made due to the 2D nature of the technique. With 3D EBSD, two key assumptions are no longer required, as additional information can be derived from the 3D map. This paper compares the benefits and limitations of 2D and 3D EBSD for twin characterisation. 2D EBSD enables a larger number of twins to be mapped in a given space of time, giving better statistics. 3D EBSD provides more comprehensive twin characterisation and will be a valuable tool for validation of 2D stereological methods and microstructural models of twinning during deformation.

Key words: EBSD; EBSP; twin; 3D microscopy; focused ion beam

Introduction

Twin characterisation plays an important role in understanding the deformation and annealing behaviour of many metals, particularly those with hcp crystal structures[1~8]. Often, the aim is to determine the volume fraction of twins within a material, perhaps as a function of strain. However, many materials twin on several different systems and form secondary or tertiary, as well as primary, twins. Furthermore, the variants of a particular twin type may be activated to differing extents. Analysis of these aspects of twinning can be critical to understanding the deformation behaviour of some materials.

Detailed twin characterisation includes a breakdown of the volume fraction of twins by:

1) generation (primary, secondary, tertiary);

2) system (family of twinning planes and directions); and

3) variant (specific plane and direction within this family).

It may also include measuring aspects of twin morphology, such as average thickness or aspect ratio, for each twin type.

The limitations of twin characterisation using techniques other than EBSD are covered well by Henrie et al[5]. Nevertheless, a brief summary is given here. With optical microscopy, twins are identified on a polished and etched cross-section on the basis of their morphology. If the sample is poorly etched, not all twins may be revealed. Distinguishing the twinned part of a grain from its parent becomes difficult with increasing strain, as the twinned part may then comprise the majority of the grain and no longer have a typical twin shape. In materials where multiple twinning systems are active, it can be difficult to differentiate one type of twin from another, although this may be done successfully at low strains in materials where the different twin types exhibit quite different morphologies. TEM enables very detailed twin characterisation, e.g. Ref. [1], but it is extremely time consuming to measure enough twins to obtain reasonable statistics using this tech-

Accepted date: 2005 - 09 - 20
E-mail: nave@hkltechnology.com

nique. Much larger volumes of material can be analysed using neutron diffraction, but information about twin morphologies and the number of active variants can not be obtained.

2D EBSD overcomes most of these limitations by simultaneously providing the crystallographic and morphological information that is needed for detailed twin characterisation and doing this over a large enough area to give the results reasonable statistical significance. As a consequence, 2D EBSD has played an important role in the analysis of the behaviour of materials that deform by twinning in recent years[2~8] and manual, semi-automatic and automatic methods for extracting twin statistics from 2D EBSD data have been developed[5, 9~12]. However, these statistics can only be extracted by making assumptions about the 3D nature of the twins and twin boundaries based on information in the 2D section. While 2D boundary analysis works well for $\Sigma 3$ boundaries in fcc materials[10], its reliably has not been tested over a wide range of materials and boundary types. With 3D EBSD, comprehensive twin characterisation can be conducted without the need to make assumptions about the third dimension. This paper compares the process of twin characterisation using 2D and 3D EBSD and discusses the benefits and limitations of the two techniques.

1 2D twin characterisation

The process of measuring the volume fraction of a particular twin type using 2D EBSD can be expressed in the following six steps:

1) Identify candidate twin boundaries based on misorientation

2) Check coincidence of twin plane normals

3) Check alignment of twin plane normals with boundary trace normal

4) Differentiate parent and twin regions

5) Calculate area fraction of twins

6) Convert area fraction to volume fraction

A summary of this process is given below, using the characterisation of {10 - 12} twins in a deformed magnesium sample as an example.

The first step is to highlight boundaries having a misorientation angle and axis that corresponds (within a selected tolerance) to that of a particular twin type. This is shown in Fig 1, where the blue boundaries are those having an 86 °〈1 - 210〉 misorientation, the parent-twin misorientation for {10 - 12} twins in magnesium. In most cases, the twin types expected in a material and the corresponding parent-twin misorientations will be known from the literature. If this is not the case, the most prevalent parent-twin misorientations in a sample can readily be identified by examining misorientation angle and axis distributions[4].

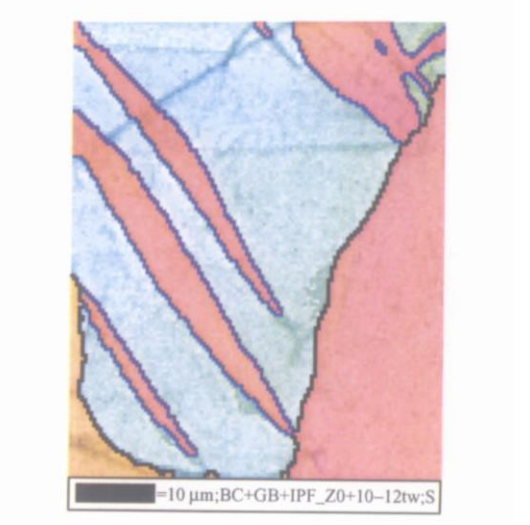

Fig 1 A small area of an EBSD map taken on a deformed magnesium alloy. Boundaries with an 86 °〈1 - 210〉 misorientation (+ / - 5 °on both angle and axis) are coloured in blue, while general grain boundaries (> 15 °) are coloured in black

If the boundaries highlighted in step 1 are indeed twin boundaries of the expected type, then the boundary plane will be the expected twin plane: (a) the crystals on either side of the boundary will have coincident twin plane normals and (b) these twin plane normals will coincide with the normal to the boundary plane. While the first criterion (a) can easily be checked using the pole figure for the twinning plane (Fig 2), the second one (b) can not be checked with certainty using a single 2D cross-section. With a single 2D cross-section, the best that can be done is to check that the coincident twin plane normals lie along the trace of the boundary normal on the 2D section (Fig 2). As will be seen later, with 3D EBSD a more rigorous test can be applied.

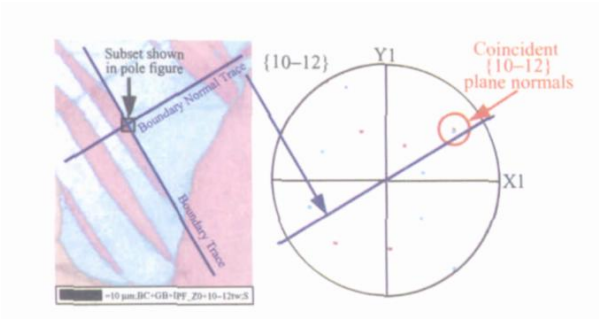

Fig 2 The {10 - 12} plane normals for the parent and twin regions coincide and lie along the trace of possible boundary plane normals

The next step requires the discrimination of parent and twin regions. In the example given here, with a low applied strain and lenticular twins, the twins can easily be identified by eye. However, at higher strains (and with nearly parallel-sided twins), this is more difficult. In these cases, it is usual to discriminate parent and twin regions based on their crystallographic orientation with respect to the imposed deformation. In simple cases (Fig. 3) a qualitative comparison may quickly reveal the parent and twin. The quantitative way to separate parent and twin regions is using their Schmid factor. While this produces good results in some circumstances, even this method has limitations[11]. Because of the inhomogeneity of deformation within a bulk sample, the stress state experienced by a particular grain may differ markedly from that imposed on the sample as a whole. Grains sometimes twin in the opposite manner to that expected from the imposed strain, possibly due to inhomogeneous deformation within the bulk but perhaps also due to the formation of twins on unloading[4, 6, 7, 13].

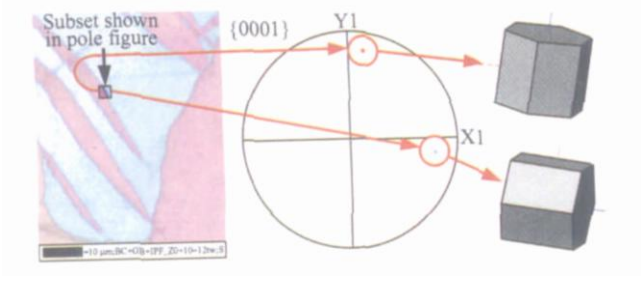

Fig 3 {10 - 12} twinning occurs in response to tension parallel to the *c*-axis of the parent grain. Therefore, the formation of twins with 〈0001〉 approximately parallel to Y1 in a parent grain with 〈0001〉 approximately parallel to X1 is compatible with tension parallel to X1.

Once parent and twin regions have been identified, the area fraction of twins can be calculated quite readily. However, the conversion from area to volume fraction is still not straightforward since the volumes of the twin and parent regions are not known. The conversion may be accomplished by making assumptions about twin and grain dimensions based on measurements made in the 2D section. This is discussed in more detail by Mason et al[11].

In summary, quite detailed twin characterisation can be carried out using 2D EBSD. Its limitations are that:

1) the coincident twin plane normals can not be checked for alignment with the boundary normal (only with the trace of the boundary normal in the section plane);

2) the selection of parent and twin regions can be uncertain, particularly at moderate to high levels of strain; and

3) assumptions have to be made in the conversion from area to volume fraction.

3D EBSD

3D EBSD is the combined use of focused ion beam (FIB) milling and electron backscatter diffraction (EBSD) to create a 3D microstructural model that includes information about crystallographic orientation[14]. The 3D model is reconstructed from a series of 2D EBSD maps taken on successive cross-sections through a material. The FIB cuts a fresh section, a 2D EBSD map is taken on that section and the process is repeated for the number of sections required for the model. The "depth" (or *Z*-dimension) of the model and the thickness (ΔZ) of each section can be chosen by the user. While the technique could theoretically be used to generate high-resolution 3D EBSD models of quite large microstructural volumes, in practice, the volume of the model and its spatial resolution (voxel size) is limited by the time needed for both EBSD mapping and FIB milling. A practical size with today's technology (taking just over 24 hours to complete) is a 20 ×20 ×20 μm volume with a 0.2 μm step size in each direction.

The 3D EBSD model presented below was acquired on an FEI Nova 600 DualBeam fitted with an HKL Nordlys II detector. Dedicated software (EBS3 from FEI) was used to coordinate the FIB milling and

EBSD mapping to enable completely automated acquisition. EBSD mapping was carried out using HKL Corona and post-processing using HKL Channel (3D-EBSD) software. More information about the acquisition process is given in Ref. [14]. A similar process could be carried out using other FIB + SEM + EBSD systems but would be much more labour intensive and time consuming due to the need to align the specimen manually after each section is milled.

2 3D Twin Characterisation

Figure 4a shows a 3D EBSD reproduction of a nickel thin-film sample with a grain size in the order of 1 μm. Just to the right of centre is a grain crossed by two twins. A volume surrounding this grain was taken as a subset (Fig. 4(b)). A grain reconstruction was then performed on this subset, with twin boundaries included as grain boundaries so that each twin or parent region was reconstructed as a separate "grain". The grain reconstruction is shown in Fig. 5, along with the orientation of each twin or parent region as a schematic unit cell and the best-fit ellipsoid for each region as a black wire-frame.

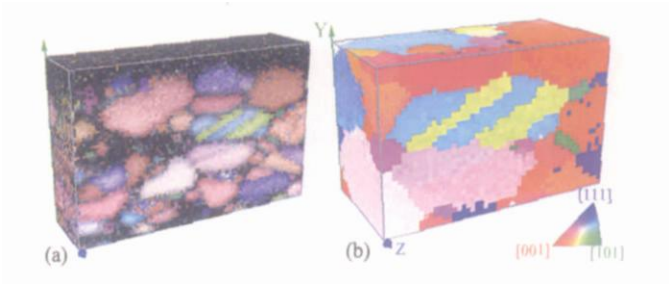

Fig. 4 3D EBSD reproduction of a thin-film nickel sample. (a) 19.4 × 12.6 × 5 μm volume consisting of cubic voxels with 0.2 μm sides. Raw crystallographic data in inverse pole figure colouring superimposed on Kikuchi band contrast. (b) 10.2 × 6.4 × 4.8 μm subset containing a twinned grain, showing data in inverse pole figure colouring after a small amount of noise reduction.

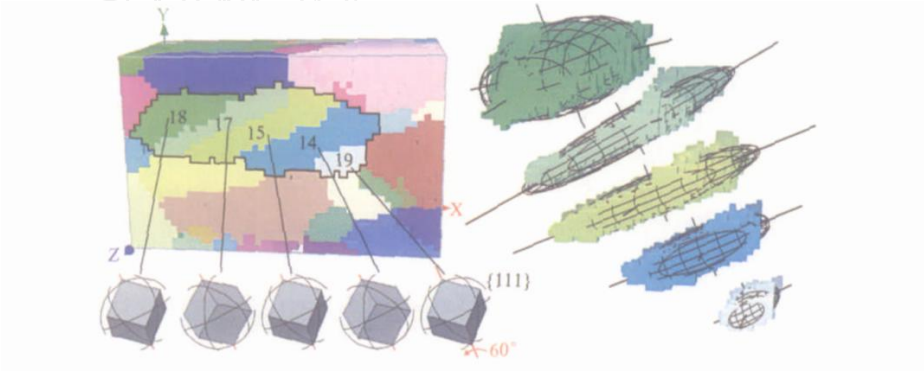

Fig. 5 Grain reconstruction of the subset in Fig. 4(b) with each grain in a different colour. Twin boundaries have been included as "grain boundaries", so that each segment of the twinned grain in the centre is reconstructed as a separate "grain". The crystallographic orientations of the segments and their best-fit ellipsoids are also shown.

Orientation data for the five regions within the twinned grain are shown in Table 1 while Table 2 presents the angles and axes of misorientation between the regions. The regions are clearly related by a misorientation very close to 60°〈111〉 in each case. This information can easily be gleaned from a single 2D EBSD map cutting through the five regions. The additional information provided by 3D EBSD comes from automatic calculation of the volume of each region and fitting of best-fit ellipsoids.

Table 1 Data for the five regions marked in Fig. 5, automatically generated during 3D grain reconstruction

Region	No. of Voxels	Volume 1000 × (μm^3)	Surface Area (μm^2)	Mean Orientation, Euler Angles (°)	Mean Misorientation (°)	Ellipsoid Radii (μm)
18	6039	50.1	0.894	91.5, 41.2, 65.0	1.326	0.313, 0.283, 0.155
17	2276	18.9	0.898	358.7, 27.4, 5.2	1.211	0.430, 0.304, 0.069
15	3240	26.9	0.926	92.4, 39.8, 64.8	0.979	0.391, 0.323, 0.070
14	2147	17.8	0.619	1.5, 27.6, 2.4	0.508	0.364, 0.240, 0.072
19	639	5.3	0.246	92.9, 40.8, 64.6	0.939	0.280, 0.099, 0.054

Note: The mean orientations are expressed relative to the sample coordinate system in this table, whereas in Ref. [14] they were expressed in raw (as acquired) form.

Table 2 Misorientations between the five regions marked in Fig. 5

Regions	Misorientation Angle (°)	Misorientation Axis (nearest low index axis)	Deviation of actual misorientation axis from nearest low index axis (°)
18 - 17	58.67	[1 - 1 - 1]	1.42
17 - 15	59.86	[1 - 11]	0.44
15 - 14	59.44	[- 111]	0.71
14 - 19	59.80	[1 - 11]	0.24

The shortest axes of the best-fit ellipsoids approximate the normals to the boundary planes between the regions. So the coincident twin plane normals for adjacent grain segments can be compared with these, rather than just with the trace of the boundary plane normals. This comparison is illustrated in Fig. 6. There is a 17° misorientation between the direction of the coincident {111} plane normals and the average direction of the shortest axis of the best-fit ellipsoids, which is close to a coincident 〈234〉 direction. This considerable deviation of the measured boundary plane from {111} could result from a few possible sources. One is the approximation of the boundary plane normals by the short-axes of the best-fit ellipsoids. A more accurate method would be to calculate boundary plane normals during the grain reconstruction process. Another possibility is that at least part of the deviation is real. Near-{111} Σ3 boundaries can accommodate considerable deviation from the {111} plane via steps in the boundary[15]. Misalignment of the 2D sections can be eliminated as a possible source of error due to the sub-pixel accuracy of the automatic alignment process used in this work[14].

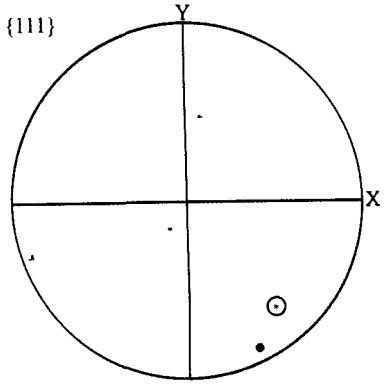

Fig. 6 {111} pole figure showing the coincident twin plane normals (circled in orange) and the average direction of the shortest best-fit ellipsoid axes for the five regions marked in Fig. 5 (red dot).

The advantages of 3D EBSD over 2D EBSD for twin characterisation are that:

1) the automatic calculation of grain segment volumes enables accurate calculation of twin volume fractions, rather than assumption-based conversion from area fractions; and

2) the coincident twin plane normals can be checked for alignment with the actual boundary normals (although in this analysis the actual normals were approximated by the shortest axes of the best-fit ellipses).

Uncertainty in the selection of parent and twin regions, particularly at moderate to high levels of strain, remains a limitation of the technique. Disadvantages compared with 2D EBSD are the need for more expensive equipment and the smaller number of twins that can be mapped in a given period of time.

3 Conclusions

EBSD is a powerful technique for twin characterisation. It enables detailed classification of twins based on generation, system, variant and morphology. This either can not be done as reliably or can not be done on a reasonable statistical basis with other techniques. 3D EBSD takes EBSD twin characterisation to the next level by enabling the boundary plane to be determined (rather than just its trace) and twin volume fractions to be calculated more accurately. Although the microstructural volumes that can currently be mapped with 3D EBSD are reasonably small, the technique is valuable for validation of stereological procedures used on 2D EBSD maps and for detailed characterisation of grain, feature or particle shape.

Acknowledgements

The authors would like to acknowledge Dr. A. P. Day for his major contribution to the development of 3D-EBSD during his time with HKL Technology and for

his contribution to the work presented in this paper.

References:

[1] Gharghouri M A, Weatherly G C, and Embury J D. The interaction of twins and precipitates in a Mg-7.7at % Al alloy [J]. Philosophical Magazine A, 1998, 78: 1137 - 1149.

[2] Salem A A, Kalidindi S R, Doherty R D. Strain hardening of titanium: Role of deformation twinning [J]. Acta Materialia, 2003, 51: 4225 - 4237.

[3] Yang P, Yu Y, Chen L, et al. Experimental determination and theoretical prediction of twin orientations in magnesium alloy AZ31 [J]. Scripta Materialia, 2004, 50: 1163 - 1168.

[4] Nave M D, and Barnett M R. Microstructures and textures of pure magnesium deformed in plane-strain compression [J]. Scripta Materialia, 2004, 51: 881 - 885.

[5] Henrie B L, Mason T A, and Hansen B L. A semiautomated electron backscatter diffraction technique for extracting reliable twin statistics [J]. Metallurgical and Materials Transactions, 2004, 35A: 3745 - 3751.

[6] Barnett M R, Nave M D, and Bettles C J. Deformation microstructures and textures of some cold rolled Mg alloys [J]. Materials Science and Engineering A, 2004, 386: 205 - 211.

[7] Barnett M R, Keshavarz Z, and Nave M D. Microstructural features of rolled Mg-3Al-1Zn [J]. Metallurgical and Materials Transactions, 2005, 36A: 1697 - 1704.

[8] Dewobroto N, Bozzolo N, Wagner F. Influence of deformation substructures on the early mechanisms of recrystallization in cold-rolled titanium and zirconium [J]. Materials Science Forum, 2005, 495 - 497: 711 - 716.

[9] Randle V. A methodology for grain boundary plane assessment by single-section trace analysis [J]. Scripta Materialia, 2001, 44: 2789 - 2794.

[10] Randle V, and Davies H. A comparison between three-dimensional and two-dimensional grain boundary plane analysis [J]. Ultramicroscopy, 2002, 90: 153 - 162.

[11] Mason T A, Bingert J F, Kaschner G C, et al. Advances in deformation twin characterization using electron backscattered diffraction data [J]. Metallurgical and Materials Transactions, 2002, 33A: 949 - 954.

[12] Henrie B L, Mason T A, and Bingert J F. Automated twin identification technique for use with electron bachscatter diffraction [J]. Materials Science Forum, 2005, 495 - 497: 191 - 196.

[13] Wonsiewicz B C, and Backofen W A. Plasticity of magnesium crystals [J]. Transactions of the Metallurgical Society of AIME, 1967, 239: 1422 - 1431.

[14] Mulders J J L, and Day A P. Three-dimmensional texture analysis [J]. Materials Science Forum, 2005, 495 - 497: 237 - 242.

[15] Randle V, Davies P, and Hulm B. Grain-boundary plane reorientation in copper [J]. Philosophical Magazine A, 1999, 79: 305 - 316.

·动态与信息·

《中国科学技术协会年鉴》(2006)开始征稿

2005年 12月 19日,《中国科学技术协会年鉴》(2006)编纂工作正式开始启动。

《中国科学技术协会年鉴》的编辑工作一直备受各位领导的关注,该书编委会主任由中国科协副主席、党组书记、书记处第一书记邓楠担任。

《中国科学技术协会年鉴》(以下简称《年鉴》)是反映中国科协系统年度工作的纪实性、史料性文献资料集,每年一集,内容主要记载上一年中国科协系统的重要工作和重点活动成果,体现中央、国务院对中国科协工作的重视和关怀,体现广大科技工作者在科协工作中的主导地位和作用,反映中国科协改革与发展的成就。旨在对内指导工作,促进工作水平的提高;对外展示形象,促进社会各方面对中国科协工作的理解和支持。《年鉴》的编辑、出版,是中国科协自身建设中的基础性工作。

为增强《年鉴》的时效性,提高《年鉴》的使用价值,及时反映科协工作情况,更好地为中国科协系统提供服务,今后《年鉴》(包括 2006年)的出版时间将调整为上半年。《年鉴》(2006)将于 2006年 5月底出版。请全国性学会、协会、研究会,各省、自治区、直辖市科协,新疆生产建设兵团科协等继续给予积极配合,于 2006年 2月 8日前提供相关稿件。

本次年鉴的编辑工作将首次由中国科协信息中心负责完成。相关信息请留意中国科协的通知通告。